
Article:

Yang, Z, Tate, JE orcid.org/0000-0003-1646-6852, Rushton, CE et al. (2 more authors) (2022) Detecting candidate high NOx emitting light commercial vehicles using vehicle emission remote sensing. Science of the Total Environment, 823. 153699. ISSN 0048-9697

https://doi.org/10.1016/j.scitotenv.2022.153699

Detecting Candidate High NO_x Emitting Light Commercial Vehicles Using Vehicle Emission Remote Sensing

Zhuoqian Yang [1*], James Tate [1], Christopher Rushton [1], Eleonora Morganti [1], Simon Shepherd [1]

[1] Institute for Transport Studies, University of Leeds, Leeds, LS2 9JT, UK

[*] Corresponding Author Zhuoqian Yang, email: tszy@leeds.ac.uk

Abstract:

Vehicle emission remote sensing devices have been widely used for monitoring and assessing the real-world emission performance of vehicles. They are also well-suited to identify candidate high emitting vehicles as remote sensing surveys measure the on-road, real-driving emissions (RDE) of a high proportion of the operational vehicle fleet passing through a testing site. This study uses the Gumbel distribution to characterise the fuel-specific NO_x emission rates (grams.kg^{-1}) from diesel vans (formally referred to as light commercial vehicles or LCVs) and screen candidate high emitting vehicles. Van emission trends of four European countries (Belgium, Sweden, Switzerland and the UK) from Euro 3 to Euro 6a/b have been studied, and the impact of road grade on candidate Euro 6a/b high-emitters is also evaluated. The measurements of Euro 6a/b fleets from four countries are pooled together, and a consistent 4% of candidate high-emitters are found in both class II and class III Euro 6a/b vans, accounting for an estimated 24% and 21% total NO_x emissions respectively. The pooled four country data is differentiated by vehicle models and manufacture groups. Engine downsizing of Euro 6a/b class II vans is suspected to worsen the emission performance when vehicles are driven under high engine load. The VW Group is found to be the manufacture with cleanest NO_x emission performance in the Euro 6a/b fleets. By distinguishing high-emitters from normally behaving vehicles, a more robust description of fleet behaviour can be provided and high-emitting vehicles targeted for further testing by plume chasing or in an inspection garage. If the vehicle is found to have a faulty, deteriorated or tampered emission after-treatment system, the periodic vehicle inspection safety and environmental performance certificate could be revoked.

Keywords: remote sensing, vans, NO_x emissions, high-emitters identification

1 Introduction

Road transport is a major contributor to nitrogen oxides (NO_x) concentrations, which has negative effects on public health and the environment (Pastorello and Melios 2016). Knowledge of the real-world vehicle emissions is important to assess the effectiveness of current control measures and substantiate future policy decisions. The discrepancy between real-world driving and type-approval emissions for passenger cars has been made clear, where real-world emissions can exceed emission limits several times for different Euro standards (Weiss *et al.* 2011; Chen and Borken-Kleefeld 2014; DfT 2016). However, only a limited amount of research (ICCT 2019a; Chen, Sun and Borken-Kleefeld 2020) has studied the real-world emission performance of vans, even though vans saw a 106.2% rise in traffic over the last 25 years (compared with 29.8% for cars and 12.8% for lorries) (DfT 2020), and was estimated to contribute 36.1% of NO_x emissions from the road traffic sector in 2019 in the UK (NAEI 2021).

Researchers have been developing different methods to monitor the real-world NO_x emissions from vehicles using laboratory (chassis dynamometer) tests (Demuynck *et al.* 2012; Moody and Tate 2017), on-board tests (portable emissions measurement systems — PEMS) (O'Driscoll *et al.* 2016; Luján *et al.* 2018), plume chasing (Wang *et al.* 2011; Lau *et al.* 2015) and remote sensing instruments (Carslaw *et al.* 2011; Chen and Borken-Kleefeld 2016). Unlike laboratory tests, PEMS or plume chasing that provide second by second emission rates (grams.sec^{-1}) over a whole driving cycle or journey for a limited number of test vehicles, remote sensing instruments un-intrusively takes a snap-shot sample of fuel-specific emission rates (grams.kg^{-1}) from a large number of vehicles in a single day (Beaton *et al.* 1995; Huang *et al.* 2018). This makes remote sensing a powerful approach for monitoring fleet emission characteristics (Carslaw *et al.* 2011; Carslaw *et al.* 2013; Chen and Borken-Kleefeld 2016; Grange *et al.* 2019) and detecting candidate high-emitting vehicles (Borken-Kleefeld 2013; Pujadas, Domínguez-Sáez and De la Fuente 2017; Huang *et al.* 2019).

When analysing remote sensing measurements some form of data aggregation is needed as a single record is insufficient to derive meaningful, statistically significant insights. The most common way to aggregate remote sensing data is to calculate the mean emission rates classified by Euro standard and fuel type (Carslaw *et al.* 2011; Chen and Borken-Kleefeld 2014), based on an assumption that the distribution of vehicle emissions is symmetrical, such as following a normal distribution. However, previous remote sensing studies (ICCT 2018; AWEL 2019; Chen, Zhang and Borken-Kleefeld 2019) have shown that vehicle

NO_x emissions are not normally distributed, rather skewed-right, making mean emission statistics less appropriate to represent a group of remote sensing measurements. Moreover, early studies often use arbitrary predetermined cut points to identify high-emitters (Pujadas, Domínguez-Sáez and De la Fuente 2017; Huang *et al.* 2019), regardless of the fact that the normal emission performance may differ in a certain campaign site. Therefore further research is considered to be needed to develop a more robust method to describe the fleet behaviour and effectively distinguish high NO_x emitters from normally behaving vehicles.

This paper uses the Gumbel distribution (explained in section 2.3) to analyse the remote sensing measurements of diesel vans. Vehicles that follow the fitted Gumbel distribution (referred to as 'on-model' vehicles) are selected to represent the emission performance of the normally behaving vehicles in the operational fleet, while the smaller and more highly emitting population which do not follow the Gumbel distribution (referred to as 'off-model' vehicles) are regarded as candidate high-emitters (Rushton, Tate and Shepherd 2021). Four European countries' (Belgium, Sweden, Switzerland and the UK) remote sensing campaigns during 2011-2019 have been selected from the CONOX project (Borken-Kleefeld *et al.* 2018a) database and an overall fleet emission trend of each country is studied. The impact of road grade on Euro 6a/b fleet in the Swiss fleet is evaluated as this dataset includes a number of measurement sites with relatively steep road gradients. Euro 6a/b fleet data from the four EU countries are then combined based on two sample Kolmogorov-Smirnov test, and a more differentiated degree of analysis by manufacture groups and models is conducted.

2 Materials and methods

2.1 The measurement principle

A vehicle emission remote sensing instrument is a monitoring system that has been widely used to estimate the real-world vehicle emissions (Beaton *et al.* 1995; Carslaw *et al.* 2011). As shown in Figure 1-a, a remote sensing system positioned at a roadside includes:

- A source & detector module which passes infrared and ultraviolet light beams through the exhaust plume of passing vehicles and together with a reflecting mirror measure the attenuation of light wavelengths. The absorption of light is directly proportional to the concentration of pollutant in the atmosphere, which includes the pollutant in the plume of the vehicle crossed and in the background. After the background pollution is subtracted, only the ratio of certain pollutant to CO_2 is reported (Bishop and Stedman 1996), as the amount of plume seen is dependent on the height of the tailpipe. Fuel-specific NO_x emission rates (in g/kg fuel burned) can then be generated based on the fuel burnt in the engine (Burgard *et al.* 2006; Carslaw *et al.* 2011).
- A speed & acceleration detector which records the instantaneous speed and acceleration of the vehicle passing by.
- A camera to capture the vehicle’s number plate so that technical characteristics (fuel type, Euro standard, make, model, etc.) of the vehicle can be retrieved from national vehicle registration databases.

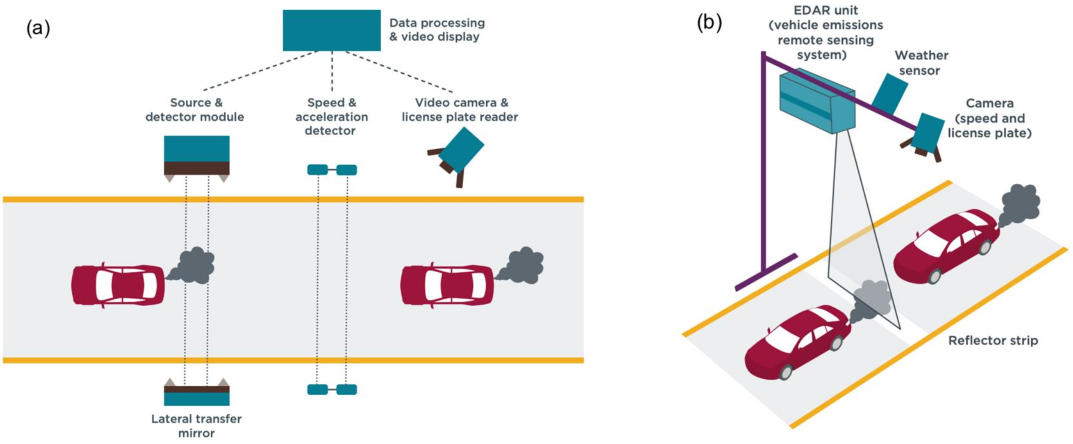

Figure 1 Schematics of a typical remote sensing deployment: (a) cross-road remote sensing system [left]; (b) top-down remote sensing system (EDAR) [right] (Borken-Kleefeld and Dallmann 2018)

An alternative configuration is the EDAR instrument which emits a sheet of laser-based infrared light in a top-down orientation, with a reflector strip mounted on the road surface scattering back the laser light (see Figure 1-b). This deployment means the measurements are less sensitive to the vehicle lane position, exhaust position and wind speed (Ropkins *et al.* 2017).

2.2 Data acquisition and preparation

Remote sensing campaigns have been conducted in Europe since the early 1990’s. In 2016, the Swiss Federal Office for the Environment (FOEN) founded the CONOX (COmbining, COmparing and COllaborating on NO_x real driving emission measurements) project, focusing on pooling, sharing, and analysing European remote sensing data collected in a range of European cities over the past 5 to 10 years (Borken-Kleefeld *et al.* 2018b; Sjödin *et al.* 2018; Borken-Kleefeld *et al.* 2018a). The remote sensing data analysed in this paper are from the CONOX project and include several remote sensing sampling campaigns carried out during 2011-2019 across Belgium, Sweden, Switzerland and the UK. As diesel vans account for 94% of van market in Europe (ICCT 2019b), this paper only considers the emission performance of vans powered by diesel. A detailed summary of fleet characteristics by country, Euro standard and class type[1] is listed in Table A. 1 in the Appendix. The number of observations from Euro 3, 4, 5 and 6a/b diesel vans accessed and analysed is 106,662.

Remote sensing data also include measurements of the testing conditions including ambient temperature, the road grade and the instantaneous speed and acceleration of each passing vehicle. The test conditions differ between countries as they are influenced by the characteristics of sample sites (road gradient, vicinity of junctions etc), driver behaviour and prevailing meteorological conditions. Based on the passing vehicles’ speed/acceleration and campaign site’s road grade, equation and parameters provided by Davison *et al.* (2020), a metric informing the instantaneous engine load called vehicle specific power (Jiménez-Palacios 1999) is calculated. Vehicle Specific Power (VSP) value is a useful metric when analysing remote sensing measurements as it characterises the power demands on the engine and associated NO_x emissions (Carslaw *et al.* 2013). It can identify vehicles under high load (where high emissions are expected) or at very low load (where fuel injection is disabled and plume sizes

---

[1] Van can be further classified into three sub-categories by reference mass, where class I are vans less than 1305kg, class II are those between 1305kg and 1760kg, and class III are those above 1760kg.

insufficient for valid remote sensing measurements) (ICCT 2018). As shown in Table A. 1 in the Appendix, the average VSP value of each fleet is much higher than the type approval NEDC[2] VSP value (around 4 kW/ton for vans). In other words, most of the vehicles (Euro 3, 4, 5 and 6a/b) being measured have higher engine load with either higher speed/acceleration or steeper road grade than the test cycle. It is hypothesised that these vehicles have been designed to have cleaner emission performance in NEDC-test-type conditions and less so for real-world conditions (Chen and Borken-Kleefeld 2014; Triantafyllopoulos *et al.* 2019).

Four remote sensing instruments, or generations of instrument, were used to conduct the remote sensing campaigns being analysed, namely the RSD series (RSD 4600 and RSD 5000) developed by Opus[3], FEAT developed by University of Denver[4], and EDAR developed by HEAT[5]. The RSD series and FEAT are cross-road remote sensing systems (shown in Figure 1-a) while EDAR is top-down remote sensing system (shown in Figure 1-b). 35.0% Switzerland samples and 22.8% UK samples were recorded by the RSD 4600 instrument which doesn't have a NO_2 measurement capability, in which case estimated NO_x ($NO+NO_2$) emission rates (grams.kg^{-1}) are generated from the measured NO and an estimated contribution from NO_2. The measurement of primary NO_2 in the exhaust has significant uncertainty and varies across remote sensing devices (Carslaw and Rhys-Tyler 2013; Chen and Borken-Kleefeld 2014; HBEFA 2019). However, in order to include samples measured by the RSD 4600 in this study, a fixed ratio of NO_2: NO_x needs to be proposed. Among two of the devices (FEAT and RSD 5000) that share the same measurement principle with RSD 4600, the FEAT device is considered to have a more robust record of NO_2 emissions compared with RSD 5000 (Carslaw *et al.* 2019), and it's measurement of NO has been proven to have a strong correlation with the RSD 4600 (Rushton *et al.* 2018). Therefore the fraction of primary NO_2 in NO_x (f_{NO2}) is directly derived from the average ratio of NO_2 to NO_x emissions measured by FEAT in remote sensing campaigns in the UK (detailed data for f_{NO2} by Euro standard and class type are listed in Table A. 2 in the Appendix) and applied to RSD 4600 measurements. Density plots of the fuel-specific NO_x emissions (grams.kg^{-1}) from both with and without NO_2 measurement capability instruments are presented in Figure 2 (Euro 6a/b is not included because all Euro 6a/b samples were measured by devices with NO_2 measurement capability). The different instruments are found to provide

---

[2] The New European Driving Cycle (NEDC) is a driving cycle used in European type-approval test. Average VSP value of NEDC cycle is also uniformly developed using the same equation and parameters, based on driving cycle's speed profile.

[3] https://www.opusrse.com/rsd-technology/

[4] http://www.feat.biochem.du.edu/

[5] https://www.heatremotesensing.com/edar

comparable NO_x emissions within the same Euro standard and class type, which suggests it is appropriate to combine records measured by different instruments into a single dataset.

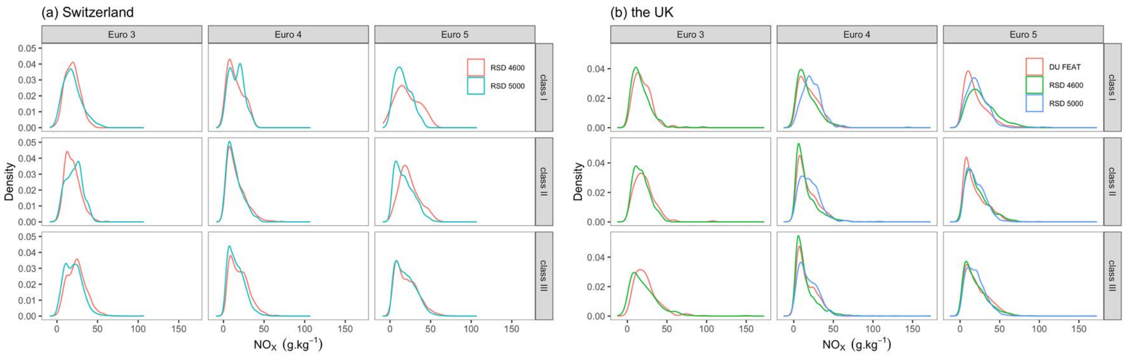

Figure 2 Density plot of NO_x emission rates (g/kg) for class I to class III vans by Euro standard and instrument in (a) Switzerland [left]; (b) the UK [right]

2.3 The Gumbel distribution and maximum R^2 value method

Figure 2 also demonstrates that the distribution of NO_x emissions measured in Switzerland and the UK has a skewed-right character and includes a proportion of extreme high emitting records. Bishop *et al.* (2016) and Huang *et al.* (2018) estimate that a small number of high-emitting vehicles could contribute a significant amount of total emissions, indicating that the emissions of the normally behaving vehicles would be elevated if simply using the mean emission statistics of a fleet. An accurate description of the remote sensing data distribution is essential in understanding the vehicle fleet behaviour. It does not only describe the average performance of the normally-behaving vehicles, but also identify candidate high-emitting vehicles.

The Gumbel distribution (Type-I Generalised Extreme Value distribution) (Gumbel 1935) is a right-skewed distribution function commonly used and widely adopted to model populations with a small number of extreme values that would not be captured by a normal distribution (Sherif *et al.* 2014; Ouarda *et al.* 2015; Bhagat 2017; Loucks and Beek 2017). Rushton, Tate and Shepherd (2021) proposes using the Gumbel distribution to characterise passenger cars' remote sensing data. As diesel vans have similar emission characteristics to diesel passenger cars (Chen, Sun and Borken-Kleefeld 2020), the Gumbel distribution has also been applied to vans in this paper. The probability density function (*pdf*) *f(x)* and cumulative density function (*cdf*) *F(x)* of a Gumbel distribution are given as:

$$f(x) = \frac{1}{b} e^{-\left(\frac{x-a}{b} + e^{-\frac{x-a}{b}}\right)} \qquad \textit{Eq. 1}$$

$$F(x) = 1 - e^{-e^{\frac{x-a}{b}}} \qquad \text{Eq. 2}$$

Where *a* is the location parameter and represents the highest observation frequency in a dataset; and *b* is the scale parameter and represents the spread of the dataset.

When describing remote sensing measurements, the Gumbel distribution is considered superior to other commonly used skewed-right distributions (Weibull, Gamma, log-normal) as:

- The parameters in the Gumbel distribution are easy to interpret. The location parameter *a* describes the emission rates that have been recorded with the most frequency and scale parameter *b* determines the statistical dispersion of the probability distribution; and
- The Gumbel distribution can be applied to negative values. In remote sensing campaigns, small negative values are sometimes recorded because of measurement noise and inaccurate determination of the background concentration (e.g. a clean vehicle with very low emissions of NO_x emissions follows with a short headway a high NO_x emitting vehicle) (Huang *et al.* 2018; Smit *et al.* 2021). These negative measurements should be included and not rounded to zero (Bishop, Burgard and Stedman 2006; McClintock 2011; Gruening *et al.* 2019), as this would artificially uplift the negative values to zero and would inflate the average values of the whole fleet.

It is hypothesised that the majority of the fleet follow the Gumbel distribution except some extreme values, and these outliers are interpreted as candidate high emitting vehicles (Rushton, Tate and Shepherd 2021). To test this hypothesis in diesel vans, the distribution is cut successively by percentile, from 99% (vehicles with the highest 1% NO_x emissions is removed from the whole fleet) to 1% (vehicles in the top 99% NO_x emissions range is removed), and the Gumbel distribution is re-applied to each sub-fleets. Then a goodness of fit test is used to calculate R^2 value of observed and theoretical quantiles for each sub-fleet after cutting. The sub-fleet with the maximum R^2 value is regarded as the ‘on-model’ vehicle subset, and its corresponding Gumbel location parameter *a* is used to represent the typical emission rate of the normally behaving vehicles in the whole fleet, while scale parameter *b* determines the dispersion of the data. The percentage of vehicles that do not follow Gumbel distribution are regarded as ‘off-model’ percentage, and these vehicles are considered as candidate high emitting vehicles. The detailed algorithm is given in Table 1.

Table 1 Algorithm for identifying the ‘off-model’ vehicles

Step 1: Apply the Gumbel distribution to the whole fleet F_{100}

Step 2: Calculate R^2 value of the observed and theoretical quantiles for fleet F_{100}

Step 3: Cut the fleet at each integer percentile starting from 99, apply the Gumbel distribution to F_i, $i = 99, 98, .., 1$

Step 4: Calculate R^2 value of observed and theoretical quantiles for fleet F_i (F_{99}, F_{98}, .., F_1)

Step 5: Repeat step 3-4 until there is no vehicle left in the fleet

Step 6: Create a dot plot of the cutting percentiles vs. the R^2 values

Step 7: Sub-fleet with the maximum R^2 value is regarded as the 'on-model' vehicle subset, and the fit parameters for the 'on-model' vehicles are the best description of the normally behaving vehicles in the whole fleet; the rest of the vehicles that do not follow Gumbel distribution are regarded as 'off-model' vehicles.

This method requires the original fleet to have a relatively large sample size, because vehicles being regarded as 'off-model' vehicles usually only make up a very small percentage of the whole fleet (Rushton, Tate and Shepherd 2021), if the sample size is too small, no useful insight would be derived from the 'off-model' vehicles. To ensure the statistical validity, the application of Gumbel distribution to class I vans is not discussed in this paper as the Class I vans only take account of 4.6% of the total measurements.

2.4 A merged dataset

Remote sensing data is often further segmented by VSP value (Carslaw *et al.* 2013), road grade (Costagliola, Costabile and Prati 2018), ambient temperature (Grange *et al.* 2019) and make/model (ICCT 2019a) to study different factors' impact on vehicle emissions. As each single country has only a relatively limited number of samples, data from different countries needs to be combined together to conduct analysis at a higher level of granularity. Here, the consistency of the NO_x emission performance across fleets is checked before pooling data from different countries. The two-sample Kolmogorov-Smirnov test (K-S test) is applied to investigate whether the NO_x emission data from the four countries share a statistically similar distribution. The two-sample K-S test is a nonparametric hypothesis test that compares empirical distributions of two samples and evaluates the largest absolute difference between the two cumulative density functions (Massey Jr 1951) (Lopes, Reid and Hobson 2007) .The test statistic D^* is given as:

$$D^* = max(|\overset{\wedge}{F_1}(x) - \overset{\wedge}{F_2}(x)|) \qquad \textit{Eq. 3}$$

Where $\overset{\wedge}{F_1}(x)$ is the empirical cumulative density function of NO_x of sample 1, and $\overset{\wedge}{F_2}(x)$ is the empirical cumulative density function of NO_x of sample 2.

For sufficiently large sample size, the critical value D_α at a 95% siginificance level is given as:

$$D_\alpha = 1.36\sqrt{\frac{1}{n_1} + \frac{1}{n_2}} \qquad \textit{Eq. 4}$$

Where: The 1.36 value is obtained from the Kolmogorov-Smirnov table (Massey Jr 1951). n_1 and n_2 are the sizes of sample 1 and sample 2 respectively.

The null hypothesis is: both samples come from a population with the same distribution. The null hypothesis is retained at significance level α if $D^* < D_\alpha$. However, when the sample size is too large (e.g. $n \geq 900$), the null hypothesis would be constantly rejected because its corresponding critical value D_α would be very small. In other words even extremely small difference between the estimate and the null hypothesis can be statistically significant ($p - values <$ 0.05) (Lin, Lucas Jr and Shmueli 2013). To illustrate this 'large-sample, small *p-values*' problem, Monte Carlo simulation was introduced into K-S test when testing whether two sample come from the same distribution. The detailed procedure is described in Table 2.

Table 2 Algorithm for illustrating 'large-sample, small *p-values*' problem in K-S test

1. Select two fleets, randomly sample *n* data points ($n = n_1 = n_2 =$ 100) from each fleet, apply K-Stest to generate the maximum difference $D^*_{100(1)}$ between these 2 fleets

2. Repeat step 1 for 1000 times, D^*_{100} can be obtained as $\{D^*_{100(1)}, D^*_{100(2)}, .., D^*_{100(1000)}\}$

3. Identify the theoretical distribution of $D^*_{(100)}$ $\{D^*_{100(1)}, D^*_{100(2)}, .., D^*_{100(1000)}\}$, estimate the typical value of D^*_{100} based on the distribution

4. Compare the typical value of D^*_{100} with its corresponding critical value D_α

5. Increase the last sample size n by 100, ($n_1 = n_2 = n =$ 200, 300, .., 1200), repeat step 1-5 until the sample size n gets to 1200

Data from the Belgium and Switzerland Euro 6a/b class III fleets were taken as an example to demonstrate the relationship between sample size and test results. Figure 3-a shows the median value of D^* (the black line in each boxplot) is higher than its corresponding D_α value (the red line) when $n \geq 900$, and Figure 3-b shows *p-value* is constantly below 0.05 when $n \geq 900$. In other words, the null hypothesis would be constantly rejected when the sample size *n* is larger than or equal to 900.

Figure 3-a shows the median *D** value is stable when the sample size $n \geq 500$. To avoid the ‘big sample’ issue, a Monte Carlo simulation at a sample size of 500 was applied on K-S test when testing if two fleets are likely from the same distribution and can be combined to one. As *D** follows a lognormal distribution (Wang, Zeng and Shao 2011), the mode value of *D** is compared with its corresponding D_α. Once confirmed that data from the two countries follow the same distribution, the two data subsets are combined and compared with the next country’s data.

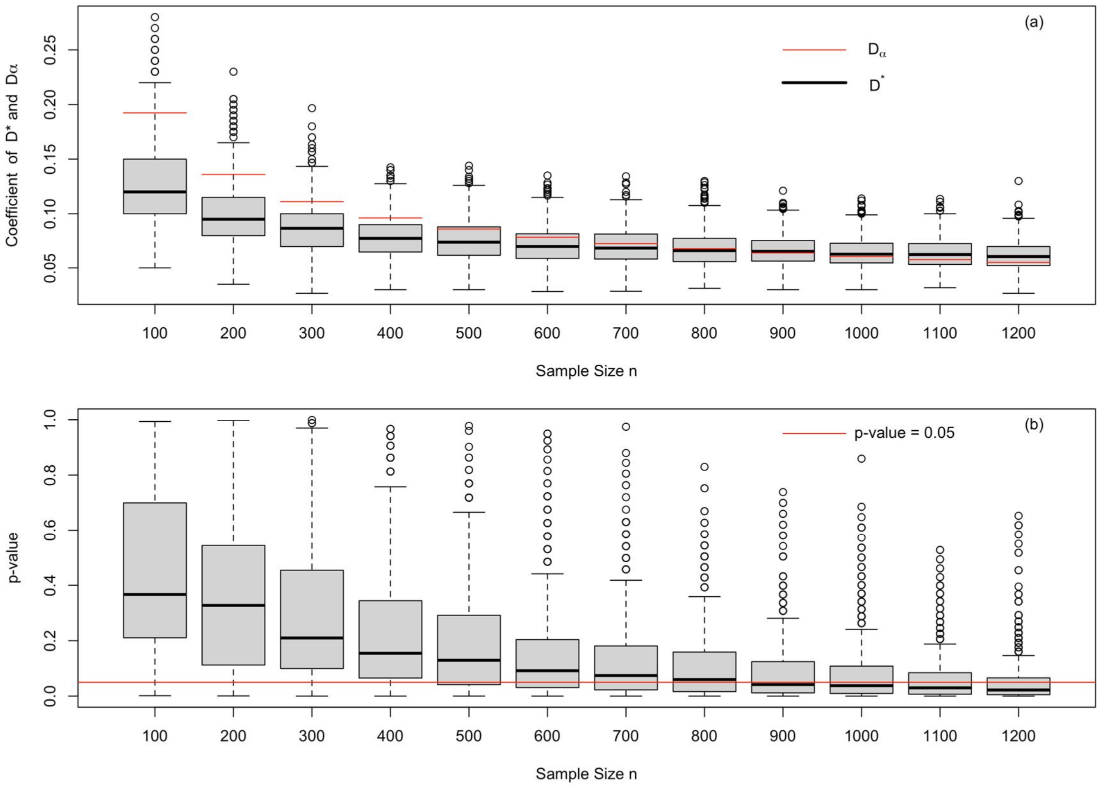

Figure 3 Distribution of (a) *D** [top panel] and (b) *p-value* [bottom panel] as a function of sample size n

3 Results and discussion

3.1 Comparison of van emission performance in four countries

The algorithm listed in Table 1 has been applied to each Euro standard and class type across four countries to identify candidate high-emitting (‘off-model’) vehicles and estimate the emission performance of normally behaving vehicles (‘on-model’) in each fleet. ‘Off-model’ percentage, ‘on-model’ vehicles’ location and scale parameters derived from the fitted distributions for each fleet are documented in Table 3. An illustrative class III Euro 5 and Euro 6a/b fleets’ R^2 value plot for each cut-off percentile is shown in Figure 4.

Table 3 ‘Off-model’ percentage and Gumbel distribution fit parameters of ‘on-model’ vehicles in Belgium, Switzerland, Sweden and the UK

		class II				class III			
	Country	**E3**	**E4**	**E5**	**E6a/b**	**E3**	**E4**	**E5**	**E6a/b**
‘Off-model’ percentage	BE	0%	1%	1%	2%	1%	1%	1%	1%
	CH	0%	0%	0%	36%	0%	0%	0%	21%
	SE	NA	0%	1%	8%	NA	0%	1%	3%
	UK	1%	0%	0%	3%	1%	1%	0%	4%
Location (g/kg)	BE	9.25	7.98	8.82	3.34	10.66	9.00	10.66	3.23
	CH	15.24	10.18	13.88	1.32	17.57	12.91	13.98	1.95
	SE	NA	9.96	12.60	2.72	NA	10.81	12.33	2.83
	UK	13.91	11.38	14.09	3.94	14.29	10.64	14.16	3.01
Scale (g/kg)	BE	5.61	5.90	6.62	4.31	6.90	6.45	7.92	4.40
	CH	7.97	7.62	9.65	2.17	9.93	8.67	10.07	2.47
	SE	NA	8.81	9.68	4.30	NA	8.66	10.43	4.92
	UK	8.67	9.25	9.67	5.31	11.24	8.69	10.13	4.62

The majority of the Euro 3, Euro 4 and Euro 5 van fleets follow the Gumbel distribution, with only 1% or 0% of ‘off-model’ vehicles identified in these fleets. The explanation for this is that the bulk of the Euro 3~5 diesel vans have high emissions, so the measurements are fitted to Gumbel distributions with relatively high location and scale parameters, as also reported for diesel cars by Rushton, Tate and Shepherd (2021). For Euro 6a/b vans, more outliers have been identified, with ‘off-model’ shares ranging from 1% to 8% for Belgium, Sweden and the UK, while Switzerland is identified to have 36% and 21% ‘off-model’ vehicles for class II and class III respectively. The majority of the Euro 6a/b fleet of vehicles are relatively clean in comparison with their predecessors, with a proportion of outliers that cannot be fitted into the Gumbel distribution and are therefore regarded as candidate high-emitting (‘off-model’) vehicles. The steep road grade at the Swiss monitoring sites is proposed as an explanation for the high share of candidate high-emitting ('off-model') in the Euro 6a/b fleet detected at these sites, and the details are provided in section 3.2.

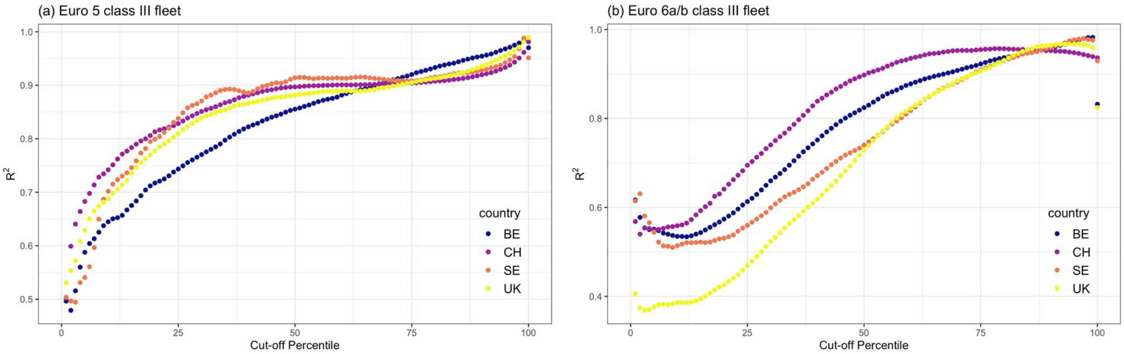

Figure 4 Variation in R^2 value as a function of cut-off percentile for (a) Euro 5 class III diesel vans [left]; (b) Euro 6a/b [right] class III diesel vans

The location parameter of Euro 3, 4, 5 and 6ab 'on-model' vehicles in the four countries are shown in Figure 5 i.e. the emission rates that have been recorded with the highest frequency in the deemed normally behaving fleet. The results for the four countries follow broadly the same trend, with the NO_x emission performance of typical vans remaining broadly stable through Euro standards 3 to 5, with emissions from Euro 5 vans slightly higher than their Euro 4 predecessors. These findings are in-line with other studies (Chen and Borken-Kleefeld 2014; ICCT 2019a). There is observed to be a significant improvement for Euro 6a/b, with an average 76.4% decrease in the fleet weighted location parameter for class III Euro 6a/b vehicles over Euro 5. The Euro 6 emission standard is more stringent with regard to the limit of NO_x (declines from 0.28 g/km (Euro 5) to 0.125 g/km (Euro 6a/b) for class III diesel vans, a reduction of 55%[6]). The implementation of Euro 6 is also directing manufactures to use more effective after-treatment system for NO_x emissions, such as selective catalytic reduction (SCR), lean NO_x trap (LNT), and exhaust gas recirculation (EGR). The integration of these NO_x control systems is observed to be leading to a considerable reduction in real-world NO_x emissions. The scale parameter fitted to Euro 6a/b is also approximately half that of Euro 5 vans' (see Table 3), demonstrating that there is not only a significant decrease in the typical NO_x emission rates, but also that the emission rates in this sub-fleet are becoming more centralized (consistent).

Test conditions (road grade, ambient temperature and VSP) have been found important to diesel van emission performance. NO_x emissions of Euro 3 to 5 vehicles in Switzerland are relatively high as the remote sensing campaigns

---

[6] Regulation (EC) 715/2007

carried out during 2011 to 2015 were at a site with a steep road grade (9%), and higher road grade is known to elevate NO_x emissions (Costagliola, Costabile and Prati (2018)). The Euro 6a/b 'on-model' van emissions in Switzerland are however low in comparison with other countries, on account of only two third of the vehicles are regarded as 'on-model' vehicles (reason discussed in section 3.2). The typical NO_x emissions of Euro 5 and Euro 6a/b in the UK are considered relatively high and it may be associated with their low ambient temperatures. Remote sensing campaigns carried out in the UK in 2017 and 2018 were in wintertime (around 10°C), during which 63% and 100% of Euro 5 and Euro 6a/b vehicles were measured. Studies (Sjödin *et al.* 2017; Grange *et al.* 2019; ICCT 2019a) have found out that light-duty diesel NO_x emissions are highly dependent on ambient temperature, with low temperature elevating NO_x emissions. However, these studies also indicate that the temperature dependence is significant for Euro 5 and Euro 4, but less so for Euro 6a/b fleet. Belgium has relatively low NO_x emissions despite its high VSP values and high certificated CO_2 emissions. The Belgium measurements were all made on a highway with an average vehicle speed of more than 70km/h, hence high VSP levels for drive-through measurements associated with aerodynamic drag and rolling resistance at these speeds. This finding is also observed in PEMS tests of Euro 5 and Euro 6a/b diesel cars, where vehicles in motorway driving conditions emit less NO_x than those on sections of urban areas (O'Driscoll *et al.* 2018). It is hypothesised that high and sustained speed would also provide enough temperature for the NO_x emission control system (e.g. EGR and SCR) commonly deployed to maintain their high efficiency operating temperature (Yang *et al.* 2021; Ntziachristos *et al.* 2016).

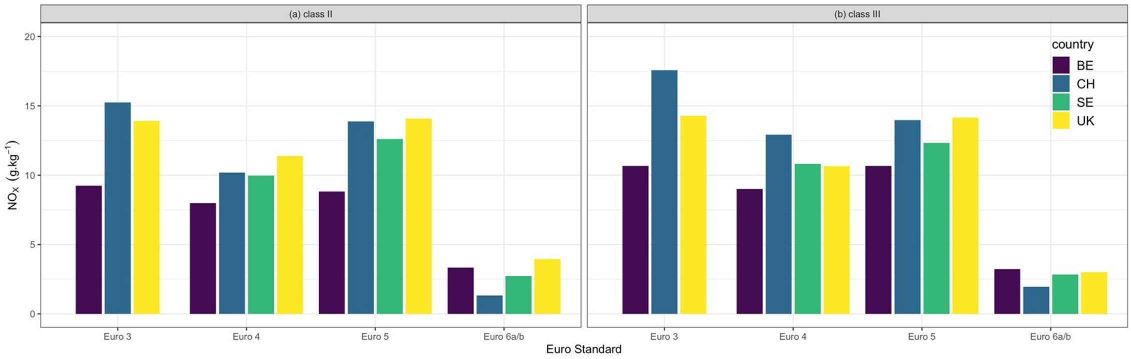

Figure 5. Typical NO_x emission rates (g/kg) for normally behaving (a) class II [left] and (b) class III [right] diesel vans by Euro standard and country

3.2 Impact of road grade on candidate high NO_x emitting vans

Recent remote sensing campaigns in Switzerland (year 2016~2019) were carried out at six sites with road grades ranging from 2.4% to 9.4%. It is hypothesised that the high percentage of 'off-model' vehicles found in Swiss Euro 6a/b fleet may be related to the steep road grade at some of the campaign sites. Data from Euro 6a/b class II and class III fleet in the Switzerland are classified by road grade and Gumbel distributions fitted and 'off-model' fractions estimated using the maximum R^2 value method (see Table A. 3 in the Appendix). The results illustrate that sites with steeper road grade (4.4% and 9.4%) have a much higher percentage of 'off-model' vehicles, which may partly explain why there are more 'off-model' vehicles identified in the Swiss Euro 6a/b fleet.

Figure 6 presents the 'on-model' vehicles in Euro 6a/b class II and class III fleets (see the orange triangular dots in Figure 6-a and Figure 6-b). NO_x emission rates in sites with relatively gentle slopes (site 1, site 2 and site 3) are higher than uphill sites (site 4, site 5 and site 6). The trend is contrary to findings for Euro 5 vehicles (refer to the blue triangular dots in Figure 6-a and Figure 6-b), where higher road grade would lead to elevated NO_x emissions (Costagliola, Costabile and Prati 2018). This is considered to be because SCR system equipped on Euro 6a/b vans can achieve better NO_x reductions when the exhaust temperature is high enough (Moody and Tate 2017). When Euro 6a/b vehicles are driven on steep road grade site, the consequent high engine load would result in better effective conversions and catalytic reductions in the SCR system and that may offset the emission increase caused by higher engine load (higher road grade).

Rushton, Tate and Shepherd (2021) found that candidate high-emitting vehicle sub-fleets also follow the Gumbel distribution, so vans being classified as 'off-model' vehicles in Swiss Euro 6a/b fleet are also fitted to the Gumbel distribution (results documented in Table A. 3 in the Appendix). The location value of each sub-fleet are regarded as the typical NO_x emission rates of the high emitting vehicles, and illustrated as orange circle dots in Figure 6-a and Figure 6-b (Euro 5 fleet doesn't have 'off-model' vehicles). In steep road grade (4.4% and 9.4%), the difference between 'on-model' vehicles and 'off-model' vehicles for Euro 6a/b class II vehicles is larger than Euro 6a/b class III vehicles. The results therefore suggest that the NO_x performance of class II Euro 6a/b vans deemed high-emitters are more sensitive to road grade compared with their class III counterparts. Considering these class II and class III fleets were measured in the same driving conditions, the difference in emission performance may be caused by different vehicle characteristics and performance of their respective exhaust after-treatment systems. However, based on the vehicle make/model information in the remote sensing database and further after-treatment system information (documented in Table A. 4 in the Appendix) extracted from the ADAC[7] vehicle catalogue or corresponding van brochures, it is found that the almost all popular models (the top-ten most commonly observed) in Euro 6a/b class II and class III vans in Switzerland are equipped with SCR systems, so the relatively poorer emission characteristics of class II vans is not found to be attributed to the type of after-treatment technology, rather their performance in the driving characteristics at this site. Further analysis of the difference between class II and class III in Euro 6a/b fleets is conducted in the next section.

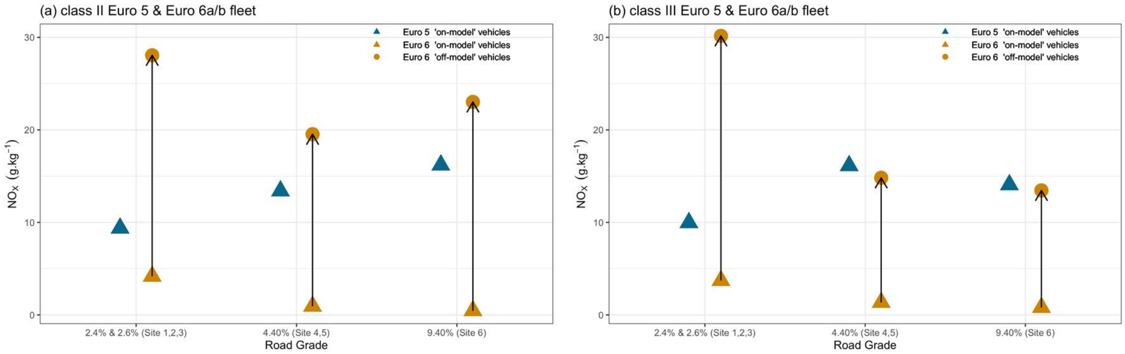

Figure 6 Impact of road grade on the typical NO_x emission rates (g/kg) of 'on-model' and 'off-model' vehicles as a function of road grade in Switzerland for sub-fleets (a) class II Euro 5 & Euro 6a/b [left]; (b) class III Euro 5 & Euro 6a/b [right] (note there are no 'off-model' vehicles in Euro 5 fleet)

It's more likely that these 'off-model' vehicles only temporarily emit high rates of NO_x at sites with steep uphill road gradients, rather than they are indeed high-emitters and can be more effectively identified on a steeper road, otherwise the same percentage of 'off-model' vehicles would probably be identified at other sites with lower road grade. Accordingly, if the purpose is to have an emission evaluation of typical vehicles in more normal operating conditions, it is advised that remote sensing campaigns be conducted at sites with a gentle slope.

3.3 The NO_x performance of normally behaving Euro 6a/b vans by vehicle model and manufacture group

To further investigate Euro 6a/b vans' emission performance, remote sensing data can be segmented by models or manufacturing groups ("families") (ICCT 2019a). However, further breaking down the fleets within one country and analysing its characteristics will not derive any useful conclusion as the sample size is too small, rather the remote sensing data across different countries needs

---

[7] https://www.adac.de/

to be combined together. To test if the four countries' data can be merged into one bigger dataset, a two sample K-S test explained in section 2.4 is applied. The result shows that for Euro 6a/b class II vans' remote sensing measurements: Belgium, Sweden and the UK follow the same distribution and can be combined into a single dataset. For Euro 6a/b class III vans' remote sensing measurements: all four countries are found to be from the same distribution and can be combined to a single dataset. After combining data from three countries in class II fleet and four countries in class III fleet, the Gumbel distribution and maximum R^2 method is applied to two fleets. A 4% of 'off-model' vehicles is found for each fleet. For class II Euro 6a/b vans, the 4% 'off-model' vehicles accounts for 24% of total NO_x emission, while the 4% 'off-model' vans in Euro 6a/b class III fleet accounts for 21% of total NO_x emission. The Gumbel distribution fitted to both the 'on-model' and 'off-model' vehicles is documented in see Table 4. The typical emission rate (location value) for class II vans are slightly higher than class III vans, with a greater spread in the distribution (higher scale value). When analysing the vehicle characteristics, no significant difference is found between 'on-model' and 'off-model' vans (shown in Table 4), except that the average engine size of class II 'off-model' vans is lower than the 'on-model' vans.

Table 4 Gumbel distribution fit parameters and fleet characteristics of 'on-model' and 'off-model' vans in merged Euro 6a/b dataset

	Class II (BE, SE, UK)		**Class III (BE, CH, SE, UK)**	
	'On-model'	**'Off-model'**	**'On-model'**	**'Off-model'**
Sample size (n)	5120	214	15777	658
Location parameter(g/kg)	3.30	33.24	3.00	29.36
Scale parameter (g/kg)	4.50	5.87	4.33	4.34
Fit R^2	97.51%	97.97%	97.23%	97.98%
Vehicle age (year)	1	1	1	1
Certificated CO_2 emission (g/km)	130	131	185	184
Engine size (cm^3)	1698	1554	2106	2083
Rated power (kW)	77	76	107	105
Curb weight (kg)	1505	1493	2139	2169

Engine downsizing is a technology to improve fuel efficiency for lighter vehicles by reducing the frictional losses and relative weight of the engine (and total kerb-weight), while the turbocharger helps provide the levels of power demanded

(Manzie 2010). While reducing CO2 emissions, a downsized diesel engine is found to increase NO_x (Johnson 2009). Payri *et al.* (2014) assesses the diesel engine downsizing limitation related to heat losses and turbocharger efficiency reduction, which suggests it might be associated with excessive emissions. However, there is no research related to engine downsizing problem of Euro 6a/b light-duty vehicles.

To test whether engine size has an impact on NO_x emissions, the merged class II and class III fleet are split into different sub-fleet by models and makes. Table A. 5 in the Appendix listed the top 5 popular models for class II and class III Euro 6a/b vans, and its corresponding Gumbel distribution fit parameters for the 'on-model' vehicles, as well as every model's engine size and vehicle rated power. All the models listed are equipped with SCR after-treatment system[8], which indicates that the type of NO_x control system is not the reason for the different emission performance between models. kW/litre specific power is introduced to represent the power density, with a higher kW/litre being characteristic of a downsized engine. Figure 7 demonstrates that the kW/litre specific power of top 5 models in class II Euro 6a/b fleets are more spread over compared with models in class III fleets. Transit Connect with the highest kW/litre specific power in class II fleet has much higher NO_x emissions. However, that's not the case for large class III Euro 6a/b vans, where both NO_x emissions and the kW/litre specific power of class III Euro 6a/b vans are relatively stable.

It is suspected that when the engine gets too small relative to the vehicle size and weight, and is driven in a relatively aggressive manner, the engine turbo-charging may not be capable of maintaining the engine power, resulting in worse fuel economy and NO_x emissions. Given the complexity of engine specifications, further investigation is required by conducting additional laboratory tests to fully appreciate the reasons behind the suspected excessive NO_x emissions from engine down-sizing. During the test NO_x emissions will be measured using a constant volume sampling system connecting with a gas analyser while engine load being tested in an engine test bench (Gao *et al.* 2019).

---

[8] https://www.adac.de/

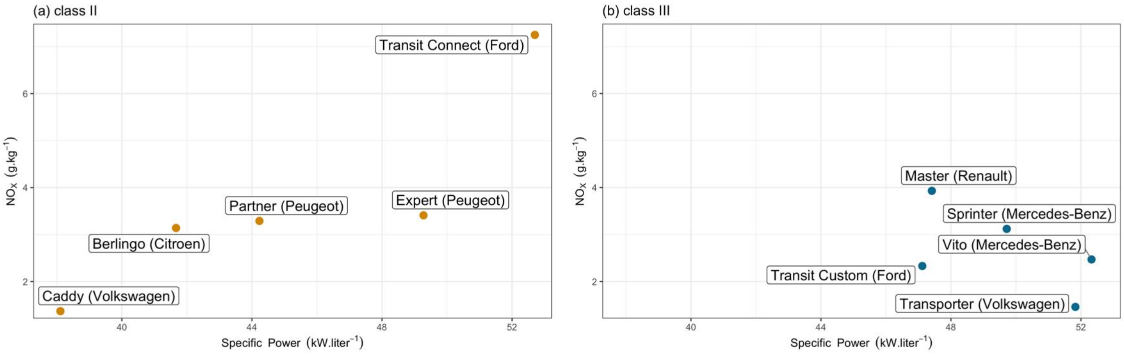

Figure 7 Relationship between kW/litre specific power and NO_x emissions (g/kg) for popular models in Euro 6a/b merged fleet: (a) class II [left]; (b) class III [right]

Merged class II and class III Euro 6a/b diesel vans are also segmented by manufacture groups, and then applied to the Gumbel distribution and maximum R^2 value cutting method. Table A. 6 in the Appendix lists 8 popular manufacture groups and their respective brands, which cover over 98% of the remote sensing measurements. Table A. 7 in the Appendix lists the detailed results of the Gumbel distribution fit parameters of 'on-model' vehicles for all the popular manufacture groups. Figure 8 presents the fuel-specific NO_x emissions of 'on-model' vehicles in each manufacture group, ordered by descending NO_x emissions. The width of the bar is the corresponding sample size of a specific manufacture group.

For the most part, manufacture group performance of class III vans is in line with the ICCT (2019a) report, as the number of class III vans out number class II vans by 3 times. The emission contribution from Class III van therefore dominates the overall trend of the van fleet. NO_x emissions vary considerably by manufacture group, and even within the same manufacture group between the performance of class II and class III vans. Daimler and Ford are found to have the worst NO_x emission performance in class II vehicles, while their class III vehicles emissions are within the average range. On the other end of the scale, the PSA Group vehicles are relatively clean in class II vehicles but are identified as the third-highest emitting manufacture in class III vehicles. The VW Group is the manufacture with cleanest NO_x emission performance of both class II and class III vehicles.

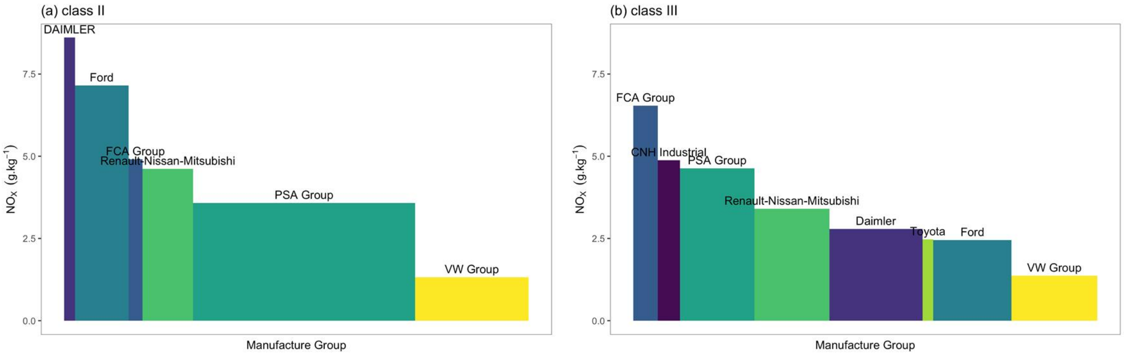

Figure 8 NO_x emissions (g/kg) by popular manufacture groups in Euro 6a/b merged fleet: (a) class II [left]; (b) class III [right] (the width of the bar is the corresponding sample size)

4 Summary and conclusions

The distribution of diesel van fuel-specific NO_x emissions in g/kg measured by remote sensing is skewed-right. To accurately characterize van emission performance and find the cut-off point for candidate high-emitters, the Gumbel distribution is applied to vehicle emission remote sensing data from four countries. Vehicles that follow the Gumbel distribution are selected to represent the emission performance of the normally behaving vehicles in a fleet, while the vehicles that do not follow the Gumbel distribution are regarded as candidate high emitting vehicles. Euro 5 and older vehicles can be fully described by the Gumbel distribution while a proportion of candidate high-emitters are identified in the Euro 6a/b fleets. The emphasis of this paper is examining the emission performance of the normally behaving vehicles and candidate high-emitters in Euro 6a/b fleet, and the key findings are:

- When comparing the fuel-specific NO_x emissions of the normally behaving vans, a reduction of emissions has only been seen since the introduction of Euro 6a/b standard vehicles, where the emissions is less than one third of the emissions from Euro 5 vans.
- A much higher percentage of ‘off-model’ Euro 6a/b vans has been observed at the measurement sites in Switzerland that had a steeper road grade, and it’s more likely that vehicles at these sites only temporarily emit high rates of NO_x. Based on this it is recommended to conduct remote sensing campaigns at a site with a gentle slope, so the assessment of the vehicles’ emission performance surveyed is in typical driving/operating conditions across a city/region/country.
- Euro 6a/b vans with improved NO_x after-treatment system (e.g. SCR) can offset the emission increasing caused by high VSP or steep road grade, as high engine load can provide enough exhaust emission temperature for the after-treatment system to work efficiently.
- After combining data from three countries in class II fleet and four countries in class III fleet, a consistent 4% of candidate high-emitters are found in both class II and class III merged Euro 6a/b vans, estimated to account for 24% and 21% total NO_x emissions respectively.
- Differentiating the cross-country merged data by models and analysing the relationship of kW/litre and emissions, illustrates that Euro 6a/b Class II vans are more sensitive to engine size. Rather than attributing the reason to different application and design of emission after-treatment systems, it’s considered more likely to be due to the engine downsizing of smaller class II vans.

- The merged data are also segmented by manufacture group. The VW Group is identified as the manufacture with the cleanest emission performance in both class II and class III Euro 6a/b vehicles. Daimler and FCA Group emit most in class II and class III Euro 6a/b fleet respectively.

This paper analyses the real-world emission performance of diesel Euro 6a/b vans, whose type approval test were being conducted under the NEDC drive cycle. The NEDC drive cycle has many cruise and mild acceleration driving conditions, which cannot represent the more dynamic driving that occur when vehicles are recorded by remote sensing device. To establish a more representative pollution test for light-duty vehicles (cars and vans), a new real-driving emissions (RDE) test procedure was introduced in 2017, and will apply to all new vans by the beginning of 2022[9]. ICCT (2019a) found the vast majority of remote sensing measurements are within normal operating conditions defined in the European RDE regulation. As a result the new Euro 6d-temp and Euro 6d vans with on-road testing are expected to have lower NO_x emissions where emission control systems can operate properly. It is recommended the analytical approach presented in this to identify candidate high-emitters is applied to emerging remote sensing datasets that have significant shares of Euro 6d-temp and Euro 6d vans, to ascertain whether this generation of vehicles have consistently low NO_x emissions, or whether a share of these vehicles with poorer emission performance make a substantial contribution to the total emissions from this sub-fleet.

The EU has founded a project called CARES[10] focusing on using contactless and un-intrusive technologies to monitor and enforce improvements in road vehicle emissions, this includes the application of roadside sampling (remote sensing and point sampling devices) and plume chasing (Pöhler *et al.* 2019). In the future, measurement data from a remote sensing device may communicate with other systems and technologies[11] for market surveillance and enforcement purposes, working towards maintaining a fleet that are in compliance with emission standards. It is suggested the Gumbel distribution could help to characterize the emission performance of the normally-behaving vehicles as well as screen high-emitting vehicles. At local levels, authorities could use the Gumbel distribution to determine the ‘cut-points’ that will help to identify high-emitting vehicles and clean vehicles. For example, a single, high instantaneous recording may not necessarily mean a vehicle consistently emits at an excessive rate but if a vehicle has two remote sensing recordings above threshold, it may be identified as a

---

[9] Commission Regulation (EU) 2017/1151

[10] https://cordis.europa.eu/project/id/814966

[11] https://cares-project.eu/

candidate high-emitter and further investigated by plume chasing (Pöhler *et al.* 2019) and/or the registered keeper is directed to get the vehicle tested at an authorized emission testing centre such as garage inspection (Huang *et al.* 2018). At a state level, the government could use the Gumbel distribution to characterize the emission performance of a vehicle family, and identify high-emitting vehicle manufactures or models.

Acknowledgements

This study has benefited greatly from the use of the CONOX db (Borken-Kleefeld *et al.* 2018a). The CONOX project focusing on pooling, sharing, and analysing European remote sensing data collected in a range of European cities. The authors would like to acknowledge the support from the CARES project (H2020 Grant Agreement no 814966). The authors are grateful to Åke Sjödin (IVL Sweden), BORKEN-KLEEFELD Jens (IIASA Austria) and Stefan Hausberger (TU Graz Austria), for providing their insightful comments on our manuscript. Zhuoqian Yang acknowledges the support of the Great Britain-China Educational Trust.

5 Appendix A. Supplementary data

Table A. 1 Summary of remote sensing fleet characteristics and test conditions in Belgium, Switzerland, Sweden and the UK

		Class I				Class II				Class III			
	Country	E3	E4	E5	E6a/b	E3	E4	E5	E6a/b	E3	E4	E5	E6a/b
Fleet characteristics													
Measurement instrument and year	BE	EDAR: 2019											
	CH	RSD 4600: 2011~2015; RSD 5000: 2016~2019											
	SE	RSD 5000: 2016, 2018											
	UK	RSD 4600: 2013,2015; RSD 5000: 2017,2018; FEAT: 2012,2013,2017,2018											
Sample size(n)	BE	106	414	484	434	263	1016	2257	2700	389	2040	7812	7361
	CH	137	135	122	164	576	1288	2427	883	3894	9956	16616	4233
	SE	12	24	22	NA	91	243	1035	1212	132	422	1772	1919
	UK	305	866	1513	201	599	3478	7030	1422	392	3227	12098	2940
Average vehicle age (years)	BE	15	10	5	1	14	10	5	1	15	10	5	1
	CH	13	10	4	2	12	8	5	2	13	8	5	2
	SE	12	7	4	NA	12	7	3	1	12	7	3	1
	UK	9	6	3	1	9	6	3	1	9	6	3	1
Certificated CO2 emission (g/km)	BE	146	135	121	113	210	183	149	132	252	228	207	186
	CH	154	136	117	115	147	158	140	129	221	234	212	185
	SE	NA	131	111	NA	155	151	140	118	232	226	204	173
	UK	128	129	122	101	155	168	156	130	219	219	207	184
Test conditions													
Ambient temperature (°C)	BE	22.5	22.7	23.0	22.2	22.5	22.6	22.9	23.2	22.5	22.5	22.9	23.0
	CH	22.8	21.2	23.6	24.5	20.7	22.3	23.4	25.1	21.2	22.0	23.4	25.2
	SE	19.2	19.9	22.9	NA	20.4	19.4	19.6	21.2	21.7	21.4	20.7	21.6

	UK	17.1	14.2	12.1	10.5	17.9	14.6	11.5	10.3	17.2	14.1	11.4	10.2
Road grade (%)	BE	2.0	2.0	2.0	2.0	1.9	2.0	2.0	2.0	1.9	2.0	2.0	2.0
	CH	8.0	7.8	6.0	8.9	8.6	7.5	6.5	4.8	8.5	7.7	6.5	4.5
	SE	3.6	3.6	3.1	NA	3.3	3.3	3.3	1.6	3.2	3.2	3.2	1.2
	UK	2.6	2.2	2.1	1.4	2.4	2.3	1.9	1.8	2.4	2.0	1.8	1.6
VSP (kW/ton)	BE	18.8	15.1	14.4	16.3	16.1	17.2	16.0	15.4	15.2	17.6	15.5	15.6
	CH	16.6	15.7	14.7	17.7	15.5	14.8	14.2	12.6	15.5	14.7	13.7	11.6
	SE	9.4	12.5	11.0	NA	11.1	10.6	10.7	12.0	10.1	11.7	10.6	12.0
	UK	9.0	8.8	8.4	11.4	7.9	7.6	7.9	9.0	7.3	7.1	8.1	8.5

Table A. 2 The fraction of primary NO_2 in NO_X (f_{NO2}) by Euro standard and class type

	Class I	Class II	Class III
Euro 3	12.96%	11.36%	13.53%
Euro 4	27.94%	25.68%	28.12%
Euro 5	25.25%	21.06%	19.10%

Table A. 3 Gumbel distribution fit parameters and VSP values for ‘on-model’ and ‘off-model’ Euro 6a/b and Euro 5 vehicles by road grade in Switzerland

	Class II					**Class III**				
Road grade and Site	**Off-model percentile**	**Vehicle status**	**Sample size (n)**	**NO_X (g/kg)**	**VSP (kW/ton)**	**Off-model percentile**	**Vehicle status**	**Sample size (n)**	**NO_X (g/kg)**	**VSP (kW/ton)**
	Euro 6a/b									
2.2% & 2.4% (site 1,2,3)	11%	‘On-model’	215	4.18	9.8	2%	‘On-model’	728	3.72	9.0
		‘Off-model’	26	28.06	11.7		‘Off-model’	15	30.16	9.4
4.4% (site 4,5)	30%	‘On-model’	245	0.94	11.0	32%	‘On-model’	1623	1.36	11.8
		‘Off-model’	105	19.53	13.0		‘Off-model’	764	14.82	11.6
9.4% (site 6)	45%	‘On-model’	95	0.46	17.3	16%	‘On-model’	318	0.81	16.3
		‘Off-model’	78	23.02	19.2		‘Off-model’	61	13.46	15.7
	Euro 5									
2.2% & 2.4% (site 1,2,3)	0%	‘On-model’	387	9.38	9.6	0%	‘On-model’	2058	9.97	8.8
4.4% (site 4,5)	0%	‘On-model’	555	13.4	12.3	0%	‘On-model’	4795	16.13	11.9
9.4% (site 6)	0%	‘On-model’	1146	16.2	16.8	0%	‘On-model’	7220	14.07	16.3

Table A. 4 Popular models in Swiss Euro 6a/b class II and class III vans and corresponding after-treatment system information

Class II			**Class III**		
Model (make)	**Sub-fleet Share**	**Equipped with SCR or not**	**Model (make)**	**Sub-fleet Share**	**Equipped with SCR or not**
Caddy (Volkswagen)	40.32%	SCR	Transporter (Volkswagen)	14.85%	SCR
Kangoo (Renault)	11.33%	SCR	Vito (Mercedes-Benz)	12.10%	SCR
Transit Connect (Ford)	9.97%	SCR	Transit Custom (Ford)	10.19%	SCR
Partner (Peugeot)	7.25%	SCR	Trafic (Renault)	9.39%	SCR
Nv200 (Nissan)	5.89%	No SCR	Daily (Iveco)	6.15%	Some with SCR, some not
Doblo (Fiat)	5.66%	SCR	Master (Renault)	5.58%	SCR
Citan (Mercedes-Benz)	4.42%	No SCR	Crafter (Volkswagen)	5.25%	SCR
Combo (Opel)	4.19%	SCR	Ducato (Fiat)	5.22%	SCR
Berlingo (Citroen)	2.94%	SCR	Vivaro-B (Opel)	4.96%	SCR
Proace (Toyota)	2.15%	SCR	Transit (Ford)	2.86%	SCR

Table A. 5 'On-model' Gumbel distribution fit parameters and fleet characteristics by top 5 Euro 6a/b models

	Model (make)	**Sample size (n)**	**Sub-fleet share**	**Off-model percentile**	**Fit R^2**	**Location (g/kg)**	**Scale (g/kg)**	**Engine size (cm^3)**	**Engine power (kW)**
Class II	Caddy (Volkswagen)	1267	21.97%	1%	98.77%	1.37	2.96	1968	75
	Partner (Peugeot)	782	13.56%	2%	98.07%	3.29	4.55	1560	69
	Berlingo (Citroen)	694	12.04%	1%	97.40%	3.14	4.52	1560	65
	Transit Connect (Ford)	582	10.09%	2%	98.54%	7.25	6.80	1499	79
	Expert (Peugeot)	423	7.34%	1%	99.28%	3.41	4.31	1867	92
Class III	Transit Custom (Ford)	1812	10.79%	3%	96.86%	2.33	4.42	1995	94
	Transporter (Volkswagen)	1573	9.36%	8%	97.25%	1.46	3.17	1968	102
	Sprinter (Mercedes-Benz)	1554	9.25%	1%	98.96%	3.12	3.95	2293	114
	Vito (Mercedes-Benz)	1358	8.08%	4%	98.08%	2.47	3.40	2064	108
	Master (Renault)	1207	7.18%	1%	97.63%	3.93	5.08	2299	109

Table A. 6 List of manufacturer groups and brands

Manufacture Group	Make Name	Manufacture Group	Make Name
CNH Industrial	Iveco	PSA Group	Citroen, Opel, Peugeot, Vauxhall
Daimler	Mercedes-Benz	Renault-Nissan-Mitsubishi	Mitsubishi, Nissan, Renault
FCA Group	Fiat	Toyota	Toyota
Ford	Ford	VW Group	Man, Volkswagen

Table A. 7 ‘On-model’ Gumbel distribution fit parameters by popular Euro 6a/b manufacture group

	Manufacture group	Sample size (n)	Off-model percentile	Fit R^2	Location (g/kg)	Scale (g/kg)
Class II	PSA Group	2499	1%	98.09%	3.58	4.69
	VW Group	1277	2%	98.74%	1.32	2.90
	Ford	601	2%	98.36%	7.15	6.71
	Renault-Nissan-Mitsubishi	569	7%	97.38%	4.62	5.53
	FCA Group	158	4%	98.25%	4.91	4.53
	DAIMLER	122	1%	97.64%	8.61	8.93
Class III	Daimler	3239	2%	98.50%	2.79	3.76
	VW Group	2985	6%	97.41%	1.37	3.03
	Ford	2721	4%	97.01%	2.45	4.28
	Renault-Nissan-Mitsubishi	2608	3%	96.96%	3.40	4.52
	PSA Group	2583	1%	98.33%	4.63	5.40
	FCA Group	847	1%	98.19%	6.54	6.37
	CNH Industrial	779	1%	97.53%	4.88	6.22
	Toyota	375	12%	97.74%	2.47	3.39

6 Reference

AWEL. 2019. *Langjährige Abgasmessungen im realen Fahrbetrieb mittels Remote Sensing* [online]. [Accessed 25 March 2020]. Available from: https://awel.zh.ch/content/dam/baudirektion/awel/luft_asbest_elektrosmog/verkehr/rsd/dokumente/RSD_Bericht_2018.pdf.

BEATON, S. P., G. A. BISHOP, Y. ZHANG, L. L. ASHBAUGH, D. R. LAWSON and D. H. STEDMAN. 1995. On-road vehicle emissions: Regulations, costs, and benefits. *Science,* **268**(5213), pp.991-993.

BHAGAT, N. 2017. Flood frequency analysis using Gumbel's distribution method: a case study of Lower Mahi Basin, India. *Journal of Water Resources and Ocean Science,* **6**(4), pp.51-54.

BISHOP, G. A., D. A. BURGARD and D. H. STEDMAN. 2006. *On-Road Remote Sensing of Automobile Emissions in the Chicago Area: Year 6, September 2004* [online]. [Accessed 11 June 2021]. Available from: http://www.feat.biochem.du.edu/assets/databases/Illinois/Arlhghts/Chicago_Year_6_CRC2004.pdf.

BISHOP, G. A. and D. H. STEDMAN. 1996. Measuring the Emissions of Passing Cars. *Accounts of Chemical Research,* **29**(10), pp.489-495.

BISHOP, G. A., D. H. STEDMAN, D. A. BURGARD and O. ATKINSON. 2016. High-Mileage Light-Duty Fleet Vehicle Emissions: Their Potentially Overlooked Importance. *Environmental Science & Technology,* **50**(10), pp.5405-5411.

BORKEN-KLEEFELD, J. 2013. *Guidance note about on-road vehicle emissions remote sensing* [online]. [Accessed 11 June 2021]. Available from: https://theicct.org/sites/default/files/publications/RSD_Guidance_BorKlee.pdf.

BORKEN-KLEEFELD, J., Y. BERNARD, D. CARSLAW, Å. SJÖDIN, J. TATE, G.-M. ALT, J. DE LA FUENTE, P. MCCLINTOCK, R. GENTALA, S. HAUSBERGER and M. JERKSJÖ. 2018a. *Contribution of vehicle remote sensing to in-service/real driving emissions monitoring - CONOX Task 3 report* [online]. Swiss Federal Office for the Environment (FOEN). [Accessed 14 April 2021]. Available from: https://www.ivl.se/download/18.34244ba71728fcb3f3fa5b/1591705759730/C295.pdf.

BORKEN-KLEEFELD, J. and T. DALLMANN. 2018. *Remote sensing of motor vehicle exhaust emissions* [online]. [Accessed 11 June 2021]. Available from: https://theicct.org/sites/default/files/publications/Remote-sensing-emissions_ICCT-White-Paper_01022018_vF_rev.pdf.

BORKEN-KLEEFELD, J., S. HAUSBERGER, P. MCCLINTOCK, J. TATE, D. CARSLAW, Y. BERNARD, Å. SJÖDIN, M. JERKSJÖ, R. GENTALA, G.-M. ALT and J. DE LA FUENTE. 2018b. *Comparing emission rates derived from remote sensing with PEMS and chassis dynamometer tests-CONOX Task 1 report* [online]. Swiss Federal Office for the Environment (FOEN). [Accessed 14 April 2021]. Available from: https://www.ivl.se/download/18.34244ba71728fcb3f3fa59/1591705759529/C293.pdf.

BURGARD, D. A., G. A. BISHOP, R. S. STADTMULLER, T. R. DALTON and D. H. STEDMAN. 2006. Spectroscopy Applied to On-Road Mobile Source Emissions. *Applied Spectroscopy,* **60**(5), pp.135A-148A.

CARSLAW, D., S. BEEVERS, J. TATE, E. WESTMORELAND and M. WILLIAMS. 2011. Recent evidence concerning higher NOx emissions from passenger cars and light duty vehicles. *Atmospheric Environment,* **45**(39), pp.7053-7063.

CARSLAW, D., N. J. FARREN, J. BORKEN-KLEEFELD and Å. SJÖDIN. 2019. *Study on the durability of European passenger car emission control systems utilizing remote sensing data* [online]. Swiss Federal Office for the Environment (FOEN). [Accessed 6 August 2020]. Available from: https://www.ivl.se/download/18.4447c37f16fa0999d1924d0/1580894080250/C387.pdf.

CARSLAW, D. and G. RHYS-TYLER. 2013. *Remote sensing of NO2 exhaust emissions from road vehicles* [online]. [Accessed 11 June 2021]. Available from: https://uk-air.defra.gov.uk/assets/documents/reports/cat05/1307161149_130715_DefraRemoteSensingReport_Final.pdf.

CARSLAW, D., M. WILLIAMS, J. TATE and S. BEEVERS. 2013. The importance of high vehicle power for passenger car emissions. *Atmospheric Environment,* **68**, pp.8-16.

CHEN, Y. and J. BORKEN-KLEEFELD. 2014. Real-driving emissions from cars and light commercial vehicles – Results from 13 years remote sensing at Zurich/CH. *Atmospheric Environment,* **88**, pp.157-164.

CHEN, Y. and J. BORKEN-KLEEFELD. 2016. NOx Emissions from Diesel Passenger Cars Worsen with Age. *Environmental Science & Technology,* **50**(7), pp.3327-3332.

CHEN, Y., R. SUN and J. BORKEN-KLEEFELD. 2020. On-Road NOx and Smoke Emissions of Diesel Light Commercial Vehicles–Combining Remote Sensing Measurements from across Europe. *Environmental Science & Technology,* **54**(19), pp.11744-11752.

CHEN, Y., Y. ZHANG and J. BORKEN-KLEEFELD. 2019. When is Enough? Minimum Sample Sizes for On-Road Measurements of Car Emissions. *Environ Sci Technol,* **53**(22), pp.13284-13292.

COSTAGLIOLA, M. A., M. COSTABILE and M. V. PRATI. 2018. Impact of road grade on real driving emissions from two Euro 5 diesel vehicles. *Applied Energy,* **231**, pp.586-593.

DAVISON, J., Y. BERNARD, J. BORKEN-KLEEFELD, N. J. FARREN, S. HAUSBERGER, Å. SJÖDIN, J. E. TATE, A. R. VAUGHAN and D. CARSLAW. 2020. Distance-based emission factors from vehicle emission remote sensing measurements. *Science of The Total Environment,* **739**, p139688.

DEMUYNCK, J., D. BOSTEELS, M. DE PAEPE, C. FAVRE, J. MAY and S. VERHELST. 2012. Recommendations for the new WLTP cycle based on an analysis of vehicle emission measurements on NEDC and CADC. *Energy Policy,* **49**, pp.234-242.

DFT. 2016. *Vehicle Emissions Testing Programme: Moving Britain Ahead* [online]. [Accessed 22 July 2020]. Available from: https://assets.publishing.service.gov.uk/government/uploads/system/uploads/attachment_data/file/548148/vehicle-emissions-testing-programme-web.pdf.

DFT. 2020. *Road Traffic Estimates: Great Britain 2019* [online]. [Accessed 12 April 2021]. Available from: https://www.gov.uk/government/statistics/road-traffic-estimates-in-great-britain-2019.

GAO, J., H. CHEN, Y. LI, J. CHEN, Y. ZHANG, K. DAVE and Y. HUANG. 2019. Fuel consumption and exhaust emissions of diesel vehicles in worldwide harmonized light vehicles test cycles and their sensitivities to eco-driving factors. *Energy Conversion and Management,* **196**, pp.605-613.

GRANGE, S. K., N. J. FARREN, A. R. VAUGHAN, R. A. ROSE and D. C. CARSLAW. 2019. Strong Temperature Dependence for Light-Duty Diesel Vehicle NOx Emissions. *Environmental Science & Technology,* **53**(11), pp.6587-6596.

GRUENING, C., P. BONNEL, M. CLAIROTTE, B. GIECHASKIEL, V. VALVERDE, A. ZARDINI and M. CARRIERO. 2019. *Potential of Remote Sensing Devices (RSDs) to screen vehicle emissions* [online]. [Accessed 11 June 2021]. Available from: https://trimis.ec.europa.eu/content/potential-remote-sensing-devices-screen-vehicle-emissions.

GUMBEL, E. J. 1935. Les valeurs extrêmes des distributions statistiques. *Ann. Inst. Henri Poincaré,* **5**(2), pp.115-158.

HBEFA. 2019. *HBEFA - Handbook Emission Factors for Road Transport (Version 4.1)* [online]. [Accessed 5 August 2020]. Available from: https://www.hbefa.net/e/documents/HBEFA41_Report_TUG_09092019.pdf.

HUANG, Y., B. ORGAN, J. L. ZHOU, N. C. SURAWSKI, G. HONG, E. F. C. CHAN and Y. S. YAM. 2018. Remote sensing of on-road vehicle emissions: Mechanism, applications and a case study from Hong Kong. *Atmospheric Environment,* **182**, pp.58-74.

HUANG, Y., B. ORGAN, J. L. ZHOU, N. C. SURAWSKI, Y.-S. YAM and E. F. C. CHAN. 2019. Characterisation of diesel vehicle emissions and determination of remote sensing cutpoints for diesel high-emitters. *Environmental Pollution,* **252**, pp.31-38.

ICCT. 2018. *Determination of real-world emissions from passenger vehicles using remote sensing data* [online]. [Accessed 7 December 2018]. Available from: https://www.theicct.org/publications/real-world-emissions-using-remote-sensing-data.

ICCT. 2019a. *A comparison of light-duty vehicle NOx emissions measured by remote sensing in Zurich and Europe* [online]. [Accessed 22 July 2020]. Available from: https://theicct.org/sites/default/files/publications/ICCT_LDV_NOx_emissions_Zurich_20190628_1.pdf.

ICCT. 2019b. *European vehicle market statistics* [online]. [Accessed 5 August 2020]. Available from: https://theicct.org/sites/default/files/publications/European_vehicle_market_statistics_20192020_20191216.pdf.

JIMÉNEZ-PALACIOS, J. L. 1999. *Understanding and quantifying motor vehicle emissions with vehicle specific power and TILDAS remote sensing*. thesis, Massachusetts Institute of Technology.

JOHNSON, T. V. 2009. Diesel emission control in review. *SAE international journal of fuels and lubricants,* **1**(1), pp.68-81.

LAU, C. F., A. RAKOWSKA, T. TOWNSEND, P. BRIMBLECOMBE, T. L. CHAN, Y. S. YAM, G. MOČNIK and Z. NING. 2015. Evaluation of diesel fleet emissions and control policies from plume chasing measurements of on-road vehicles. *Atmospheric Environment,* **122**, pp.171-182.

LIN, M., H. C. LUCAS JR and G. SHMUELI. 2013. Research commentary—too big to fail: large samples and the p-value problem. *Information Systems Research,* **24**(4), pp.906-917.

LOPES, R. H., I. REID and P. R. HOBSON. 2007. The two-dimensional Kolmogorov-Smirnov test. *In: XI International Workshop on Advanced Computing and Analysis Techniques in Physics Research,* April 23-27, 2007, Amsterdam, the Netherlands. Proceedings of Science.

LOUCKS, P. and E. BEEK. 2017. *Water Resource Systems Planning and Management.*

LUJÁN, J. M., V. BERMÚDEZ, V. DOLZ and J. MONSALVE-SERRANO. 2018. An assessment of the real-world driving gaseous emissions from a Euro 6 light-duty diesel vehicle using a portable emissions measurement system (PEMS). *Atmospheric Environment,* **174**, pp.112-121.

MANZIE, C. 2010. CHAPTER THREE - Relative Fuel Economy Potential of Intelligent, Hybrid and Intelligent–Hybrid Passenger Vehicles. *In:* G. PISTOIA, ed. *Electric and Hybrid Vehicles.* Amsterdam: Elsevier, pp.61-90.

MASSEY JR, F. J. 1951. The Kolmogorov-Smirnov test for goodness of fit. *Journal of the American statistical Association,* **46**(253), pp.68-78.

MCCLINTOCK, P. M. 2011. *The Colorado Remote Sensing Program January–December 2010* [online]. [Accessed 11 June 2021]. Available from: https://downloads.regulations.gov/EPA-R08-OAR-2016-0016-0013/content.pdf.

MOODY, A. and J. E. TATE. 2017. In Service CO2 and NOX Emissions of Euro 6/VI Cars, Light- and Heavy- dutygoods Vehicles in Real London driving: Taking the Road into the Laboratory. *Journal of Earth Sciences and Geotechnical Engineering,* **7**(1), pp.51-62.

NAEI. 2021. *UK emissions data selector* [online]. [Accessed 5 July 2021]. Available from: https://naei.beis.gov.uk/data/data-selector.

NTZIACHRISTOS, L., G. PAPADIMITRIOU, N. LIGTERINK and S. HAUSBERGER. 2016. Implications of diesel emissions control failures to emission factors and road transport NOx evolution. *Atmospheric Environment,* **141**, pp.542-551.

O'DRISCOLL, R., H. M. APSIMON, T. OXLEY, N. MOLDEN, M. E. J. STETTLER and A. THIYAGARAJAH. 2016. A Portable Emissions Measurement System (PEMS) study of NOx and primary NO2 emissions from Euro 6 diesel passenger cars and comparison with COPERT emission factors. *Atmospheric Environment,* **145**, pp.81-91.

O'DRISCOLL, R., M. E. J. STETTLER, N. MOLDEN, T. OXLEY and H. M. APSIMON. 2018. Real world CO2 and NOx emissions from 149 Euro 5 and 6 diesel, gasoline and hybrid passenger cars. *Science of The Total Environment,* **621**, pp.282-290.

OUARDA, T. B. M. J., C. CHARRON, J. Y. SHIN, P. R. MARPU, A. H. AL-MANDOOS, M. H. AL-TAMIMI, H. GHEDIRA and T. N. AL HOSARY. 2015. Probability distributions of wind speed in the UAE. *Energy Conversion and Management,* **93**, pp.414-434.

PASTORELLO, C. and G. MELIOS. 2016. *Explaining road transport emissions: a non-technical guide* [online]. European Environment Agency. [Accessed 16 October 2018]. Available from: https://www.eea.europa.eu/publications/explaining-road-transport-emissions.

PAYRI, F., J. J. LOPEZ, B. PLA and D. G. BUSTAMANTE. 2014. *Assessing the limits of downsizing in diesel engines* [online]. SAE Technical Paper. [Accessed 20 May 2021]. Available from: https://doi.org/10.4271/2014-32-0128.

PÖHLER, D., T. ENGEL, U. ROTH, M. HORBANSKI, J. LAMPEL, T. ADLER and U. PLATT. 2019. Real Driving NOx Emissions and Emission Manipulations of Trucks observed with Plume Chasing. *In: Geophysical Research Abstracts.*

PUJADAS, M., A. DOMÍNGUEZ-SÁEZ and J. DE LA FUENTE. 2017. Real-driving emissions of circulating Spanish car fleet in 2015 using RSD Technology. *Science of The Total Environment,* **576**, pp.193-209.

ROPKINS, K., T. H. DEFRIES, F. POPE, D. C. GREEN, J. KEMPER, S. KISHAN, G. W. FULLER, H. LI, J. SIDEBOTTOM, L. R. CRILLEY, L. KRAMER, W. J. BLOSS and J. STEWART HAGER. 2017. Evaluation of EDAR vehicle emissions remote sensing technology. *Science of The Total Environment,* **609**, pp.1464-1474.

RUSHTON, C. E., J. E. TATE and S. P. SHEPHERD. 2021. A novel method for comparing passenger car fleets and identifying high-chance gross emitting vehicles using kerbside remote sensing data. *Science of The Total Environment,* **750**, p142088.

RUSHTON, C. E., J. E. TATE, S. P. SHEPHERD and D. C. CARSLAW. 2018. Interinstrument comparison of remote-sensing devices and a new method for calculating on-road nitrogen oxides emissions and validation of vehicle-specific power. *Journal of the Air & Waste Management Association,* **68**(2), pp.111-122.

SHERIF, M., M. ALMULLA, A. SHETTY and R. K. CHOWDHURY. 2014. Analysis of rainfall, PMP and drought in the United Arab Emirates. *International journal of climatology,* **34**(4), pp.1318-1328.

SJÖDIN, Å., J. BORKEN-KLEEFELD, D. CARSLAW, J. TATE, G.-M. ALT, J. DE LA FUENTE, Y. BERNARD, U. TIETGE, P. MCCLINTOCK and R. GENTALA. 2018. *Real-driving emissions from diesel passenger cars measured by remote sensing and as compared with PEMS and chassis dynamometer measurements-CONOX Task 2 report* [online]. Swiss Federal Office for the Environment (FOEN). [Accessed 14 April 2021]. Available from: https://www.ivl.se/download/18.34244ba71728fcb3f3fa5a/1591705759623/C294.pdf.

SJÖDIN, Å., M. JERKSJÖ, H. FALLGREN, H. SALBERG, R. PARSMO, C. HULT, M.-R. YAHYA, T. WISELL and J. LINDÉN. 2017. *On-Road Emission Performance of Late Model Diesel and Gasoline Vehicles as Measured by Remote Sensing* [online]. IVL Swedish Environmental Research Institute [Accessed 14 April 2021]. Available from: https://www.ivl.se/download/18.449b1e1115c7dca013adae8/1499086049685/B2281.pdf.

SMIT, R., S. BAINBRIDGE, D. KENNEDY and P. KINGSTON. 2021. A decade of measuring on-road vehicle emissions with remote sensing in Australia. *Atmospheric Environment,* **252**, p118317.

TRIANTAFYLLOPOULOS, G., A. DIMARATOS, L. NTZIACHRISTOS, Y. BERNARD, J. DORNOFF and Z. SAMARAS. 2019. A study on the CO2 and NOx emissions performance of Euro 6 diesel vehicles under various chassis dynamometer and on-road conditions including latest regulatory provisions. *Science of The Total Environment,* **666**, pp.337-346.

WANG, C., B. ZENG and J. SHAO. 2011. Application of bootstrap method in Kolmogorov-Smirnov test. *In: 2011 International Conference on Quality, Reliability, Risk, Maintenance, and Safety Engineering,* 17-19 June 2011, pp.287-291.

WANG, X., D. WESTERDAHL, Y. WU, X. PAN and K. M. ZHANG. 2011. On-road emission factor distributions of individual diesel vehicles in and around Beijing, China. *Atmospheric Environment,* **45**(2), pp.503-513.

WEISS, M., P. BONNEL, R. HUMMEL, U. MANFREDI, R. COLOMBO, G. LANAPPE, P. LE LIJOUR and M. SCULATI. 2011. Analyzing on-road emissions of light-duty vehicles with Portable Emission Measurement Systems (PEMS). *JRC Scientific and Technical Reports, EUR,* **24697**.

YANG, Z., J. E. TATE, E. MORGANTI and S. P. SHEPHERD. 2021. Real-world CO2 and NOX emissions from refrigerated vans. *Science of The Total Environment,* **763**, p142974.